Transport Theory and Statistical Physics, 39:192–233, 2011

ISSN: 0041-1450 print / 1532-2424 online
DOI: 10.1080/00411450.2010.533742

MOMENT ANALYSIS OF ANGULAR APPROXIMATION METHODS FOR TIME-DEPENDENT RADIATION TRANSPORT

JEFFERY D. DENSMORE[1] and RYAN G. McCLARREN[2]

[1]Computational Physics and Methods Group, Los Alamos National Laboratory, Los Alamos, New Mexico, USA

[2]Department of Nuclear Engineering, Texas A&M University, College Station, Texas, USA

We extend moment analysis, a technique developed for investigating the accuracy of discrete-ordinates spatial discretization schemes, to time-dependent radiation transport and apply it to several angular approximation methods. Specifically, we examine the diffusion approximation, the $P_{1/3}$ *approximation, and three time-dependent generalizations of the simplified* P_N *approximation: the* SP_2*,* SP_3*, and* SSP_3 *approximations. We show that all of the these methods preserve the correct flux-weighted average of* x *but not the correct flux-weighted average of* $(x - x_a)^2$*, where* x *is the spatial variable and* x_a *is an arbitrary point. We also demonstrate that, for general cross sections and large elapsed time, the error in the flux-weighted average of* $(x - x_a)^2$ *is smallest in magnitude for the* SP_2 *and* SP_3 *approximations. In addition, we present a simple improvement to the* SP_2 *approximation that allows this method to produce the correct flux-weighted average of* $(x - x_a)^2$*. We present numerical results that test this analysis. From these results, we find that the angular approximation methods with the most accurate solutions also have the most accurate values for the flux-weighted average of* $(x - x_a)^2$*. In particular, the* SP_2 *and* SP_3 *approximations are two of the most accurate methods at large elapsed times, while the improved* SP_2 *approximation is one of the most accurate methods at all times. We also observe, however, that an accurate value for the flux-weighted average of* $(x - x_a)^2$ *is not always accompanied by an accurate solution. Consequently, we conclude that an accurate flux-weighted average of* $(x - x_a)^2$ *is a necessary rather than sufficient condition for an overall accurate angular approximation method.*

Address correspondence to J. D. Densmore, Los Alamos National Laboratory, P.O. Box 1663, MS D409, Los Alamos, NM 87545, USA. E-mail: jdd@lanl.gov

Keywords: Time-dependent radiation transport, Moment analysis, Diffusion approximation, $P_{1/3}$ approximation, Simplified P_N approximation

1. Introduction

The numerical simulation of radiation transport can be computationally expensive due to a phase space of up to seven dimensions (position, angle, time, and energy). This statement is especially true for time-dependent calculations, where the expense is typically mitigated by simplifying, in particular, the dependence on the angular variable. The most well-known and widely employed angular approximation method is the diffusion approximation. However, several other techniques have been suggested as more accurate alternatives. One such method is the $P_{1/3}$ approximation, which is a modification of the P_1 equations that yields solutions that propagate at the correct speed (Olson et al., 2000). Also, Frank et al. (2007) have presented several time-dependent generalizations of the simplified P_N approximation. These methods are the Simplified P_2 (SP_2), Simplified P_3 (SP_3), and Simplified-Simplified P_3 (SSP_3) approximations.

To compare the angular approximation methods discussed previously, we consider a theoretical technique developed by Brantley and Larsen (2000) for examining the accuracy of discrete-ordinates spatial discretization schemes, known as moment analysis. This technique is based on the method of moments (Lewis, 1950), a procedure for obtaining exact expressions for spatial and angular moments of the angular flux in an infinite, homogeneous medium. Moment analysis consists of calculating the flux-weighted averages of x and $(x - x_a)^2$, where x is the spatial variable and x_a is an arbitrary point, both exactly and as determined by a particular discretization scheme. The error in the flux-weighted averages corresponding to the discretization scheme can then be used to quantify the accuracy of the scheme as a function of the spatial mesh and material properties. Although restricted to infinite, homogeneous media, moment analysis is otherwise general in the sense that it doesn't require a sufficiently refined spatial mesh in order to be valid, as does standard truncation analysis.

In this paper we extend this moment analysis technique to time-dependent radiation transport and apply it to the aforementioned angular approximation methods. Moment analysis is especially appropriate for investigating the accuracy of these methods as they do not represent a sequence of increasingly accurate angular discretizations and consequently are not amenable to truncation analysis. We will show that all of the angular approximation methods preserve the correct flux-weighted average of x but not the correct flux-weighted average of $(x - x_a)^2$. We will further demonstrate that, for general cross sections and large elapsed times, the error in this latter quantity is smallest in magnitude for the SP_2 and SP_3 approximations, and thus we expect these two methods to be the most accurate in this regime. In addition, we will present a simple modification of the SP_2 approximation that allows this method to produce the correct flux-weighted average of $(x - x_a)^2$. Presumably, this improved SP_2 approximation should be more accurate than any of the other angular approximation methods.

We begin the remainder of this paper by developing exact expressions for the flux-weighted averages of x and $(x - x_a)^2$ in the case of time-dependent radiation transport. We then determine these same quantities for the diffusion, $P_{1/3}$, SP_2, SP_3, and SSP_3 approximations. Next, we compare the errors in the flux-weighted average of $(x - x_a)^2$ for each angular approximation method. After this comparison, we present our improved SP_2 approximation. We then test our theoretical predictions with several numerical examples. We conclude with a brief discussion.

2. Moment Analysis of the Analytic Transport Equation

We consider monoenergetic, planar-geometry, time-dependent radiation transport in an isotropically scattering, source-free, infinite, homogeneous medium. This process is modeled by the following transport equation,

$$\frac{1}{v}\frac{\partial \psi}{\partial t} + \mu \frac{\partial \psi}{\partial x} + \Sigma_t \psi = \frac{\Sigma_s}{2} \int_{-1}^{1} \psi(x, \mu', t)\, d\mu', \tag{1}$$

and boundary conditions,

$$\lim_{|x|\to\infty} \psi = 0. \tag{2}$$

Here, $-\infty < x < \infty$ is the spatial variable, $-1 \leq \mu \leq 1$ is the angular variable, $t > 0$ is the the temporal variable, $\psi(x, \mu, t)$ is the angular flux, Σ_t is the total cross section, Σ_s is the scattering cross section, and v is the particle speed. Two other important quantities are the scalar flux,

$$\phi(x, t) = \int_{-1}^{1} \psi(x, \mu, t)\, d\mu, \tag{3}$$

and the absorption cross section,

$$\Sigma_a = \Sigma_t - \Sigma_s. \tag{4}$$

Along with Eqs. (1) and (2), we also prescribe an isotropic initial condition of the form

$$\psi(x, 0, \mu) = \frac{\Phi(x)}{2}, \tag{5}$$

where Φ is the initial scalar flux. We require that Φ vanish rapidly enough as $|x| \to \infty$ such that Eq. (2) is satisfied.

We are interested in calculating the flux-weighted averages of x,

$$\langle x \rangle_\phi(t) = \frac{\displaystyle\int_{-\infty}^{\infty} x\phi(x, t)\, dx}{\displaystyle\int_{-\infty}^{\infty} \phi(x, t)\, dx}, \tag{6}$$

and $(x - x_a)^2$, where x_a is an arbitrary point,

$$\left\langle (x - x_a)^2 \right\rangle_\phi(t) = \frac{\displaystyle\int_{-\infty}^{\infty} (x - x_a)^2 \phi(x, t)\, dx}{\displaystyle\int_{-\infty}^{\infty} \phi(x, t)\, dx}. \tag{7}$$

These two expressions are time-dependent generalizations of the center of mass and squared radius of gyration, respectively, defined by Brantley and Larsen (2000). To proceed, it will be useful to define the following spatial and angular moments of the angular flux,

$$\phi_k(x,t) = \int_{-1}^{1} P_k(\mu)\psi(x,\mu,t)\,d\mu, \tag{8}$$

and

$$\begin{aligned}\phi_{m,k}(t) &= \int_{-\infty}^{\infty} x^m \phi_k(x,t)\,dx \\ &= \int_{-\infty}^{\infty}\int_{-1}^{1} x^m P_k(\mu)\psi(x,\mu,t)\,d\mu\,dx.\end{aligned} \tag{9}$$

Here, $P_k(\mu)$ is the Legendre polynomial of order k (Lewis and Miller, 1993). By comparing Eqs. (3) and (8) and using the fact that $P_0(\mu) = 1$, it is clear that ϕ_0 is the scalar flux. Then, we can combine Eqs. (6), (7), and (9) to write

$$\langle x\rangle_\phi(t) = \frac{\phi_{1,0}(t)}{\phi_{0,0}(t)}, \tag{10}$$

and

$$\langle (x-x_a)^2\rangle_\phi(t) = \frac{\phi_{2,0}(t) - 2x_a\phi_{1,0}(t) + x_a^2\phi_{0,0}(t)}{\phi_{0,0}(t)}. \tag{11}$$

Multiplying Eqs. (1), (2), and (5) by $P_k(\mu)$, integrating over angle, and employing Eq. (8) and the orthogonality of the Legendre polynomials gives

$$\frac{1}{v}\frac{\partial}{\partial t}\phi_k + \frac{k+1}{2k+1}\frac{\partial}{\partial x}\phi_{k+1} + \frac{k}{2k+1}\frac{\partial}{\partial x}\phi_{k-1} + \Sigma_t\phi_k = \Sigma_s\phi_0\delta_{k,0}, \tag{12}$$

$$\lim_{|x|\to\infty}\phi_k = 0, \tag{13}$$

and

$$\phi_k(x, 0) = \Phi(x)\delta_{k,0}. \tag{14}$$

In developing Eq. (12), we have additionally applied the recursion relation (Lewis and Miller, 1993)

$$\mu P_k(\mu) = \frac{k+1}{2k+1}P_{k+1}(\mu) + \frac{k}{2k+1}P_{k-1}(\mu). \tag{15}$$

Next, we define spatial moments of the initial scalar flux corresponding to Eq. (9),

$$\Phi_m = \int_{-\infty}^{\infty} x^m \Phi(x)\, dx. \tag{16}$$

When we multiply Eqs. (12) and (14) by x^m, where $m \geq 0$, integrate over space, and make use of Eqs. (9), (13), and (16), we have

$$\frac{1}{v}\frac{d}{dt}\phi_{m,k} - \frac{m(k+1)}{2k+1}\phi_{m-1,k+1} - \frac{mk}{2k+1}\phi_{m-1,k-1} + \Sigma_t\phi_{m,k} = \Sigma_s\phi_{m,0}\delta_{k,0}, \tag{17}$$

and

$$\phi_{m,k}(0) = \Phi_m\delta_{k,0}. \tag{18}$$

For $m = 0$ and $k = 0$, Eqs. (17) and (18) become

$$\frac{1}{v}\frac{d}{dt}\phi_{0,0} + \Sigma_a\phi_{0,0} = 0, \tag{19}$$

and

$$\phi_{0,0}(0) = \Phi_0. \tag{20}$$

We can solve Eqs. (19) and (20) to write

$$\phi_{0,0}(t) = \Phi_0 e^{-\Sigma_a vt}. \tag{21}$$

For $m = 0$ and $k = 1$, Eqs. (17) and (18) yield

$$\frac{1}{v}\frac{d}{dt}\phi_{0,1} + \Sigma_{\mathrm{t}}\phi_{0,1} = 0, \tag{22}$$

and

$$\phi_{0,1}(0) = 0. \tag{23}$$

Solving Eqs. (22) and (23) shows that

$$\phi_{0,1}(t) = 0. \tag{24}$$

For $m = 1$ and $k = 0$, we obtain from Eqs. (17), (18), and (24)

$$\frac{1}{v}\frac{d}{dt}\phi_{1,0} + \Sigma_{\mathrm{a}}\phi_{1,0} = 0, \tag{25}$$

and

$$\phi_{1,0}(0) = \Phi_1. \tag{26}$$

The solution to these two expressions is

$$\phi_{1,0}(t) = \Phi_1 e^{-\Sigma_{\mathrm{a}} vt}. \tag{27}$$

If we define the initial flux-weighted average of x as

$$\begin{aligned}\langle x\rangle_{\Phi} &= \frac{\displaystyle\int_{-\infty}^{\infty} x\Phi(x)\,dx}{\displaystyle\int_{-\infty}^{\infty} \Phi(x)\,dx} \\ &= \frac{\Phi_1}{\Phi_0},\end{aligned} \tag{28}$$

where the second equality follows from Eq. (16), then evaluating Eq. (10) with Eqs. (21), (27), and (28) gives

$$\langle x\rangle_{\phi}(t) = \langle x\rangle_{\Phi}. \tag{29}$$

Thus, the flux-weighted average of x is constant and equal to its initial value.

For $m = 0$ and $k = 2$, Eqs. (17) and (18) yield

$$\frac{1}{v}\frac{d}{dt}\phi_{0,2} + \Sigma_t\phi_{0,2} = 0, \tag{30}$$

and

$$\phi_{0,2}(0) = 0. \tag{31}$$

When we solve Eqs. (30) and (31), we have

$$\phi_{0,2}(t) = 0. \tag{32}$$

For $m = 1$ and $k = 1$, we obtain from Eq. (17), (18), (21), and (32)

$$\frac{1}{v}\frac{d}{dt}\phi_{1,1} + \Sigma_t\phi_{1,1} = \frac{\Phi_0}{3}e^{-\Sigma_a vt}, \tag{33}$$

and

$$\phi_{1,1}(0) = 0. \tag{34}$$

The solution to Eqs. (33) and (34) is

$$\phi_{1,1}(t) = \frac{\Phi_0}{3\Sigma_s}\left(e^{-\Sigma_a vt} - e^{-\Sigma_t vt}\right). \tag{35}$$

For $m = 2$ and $k = 0$, combining Eqs. (17), (18), and (35) gives

$$\frac{1}{v}\frac{d}{dt}\phi_{2,0} + \Sigma_a\phi_{2,0} = \frac{2\Phi_0}{3\Sigma_s}\left(e^{-\Sigma_a vt} - e^{-\Sigma_t vt}\right), \tag{36}$$

and

$$\phi_{2,0}(0) = \Phi_2. \tag{37}$$

By solving Eqs. (36) and (37), we see that

$$\phi_{2,0}(t) = \Phi_2 e^{-\Sigma_a v t} + \frac{2\Phi_0}{3\Sigma_s^2}\left[(\Sigma_s v t - 1)e^{-\Sigma_a v t} + e^{-\Sigma_t v t}\right]. \quad (38)$$

Defining the initial flux-weighted average of $(x - x_a)^2$ as

$$\langle (x - x_a)^2 \rangle_\Phi = \frac{\int_{-\infty}^{\infty} (x - x_a)^2 \Phi(x)\, dx}{\int_{-\infty}^{\infty} \Phi(x)\, dx} = \frac{\Phi_2 - 2x_a\Phi_1 + x_a^2\Phi_0}{\Phi_0}, \quad (39)$$

where the second equality is again from Eq. (16), and substituting Eqs. (21), (27), (38), and (39) into Eq. (11) allows us to write

$$\left\langle (x - x_a)^2 \right\rangle_\phi (t) = \left\langle (x - x_a)^2 \right\rangle_\Phi + \frac{2}{3\Sigma_s^2}\left(\Sigma_s v t - 1 + e^{-\Sigma_s v t}\right). \quad (40)$$

This expression is a statement that the flux-weighted average of $(x - x_a)^2$ is equal to its initial value plus a term that describes how particles spread out from their initial positions. Of course, this term is an increasing function of time.

Equations (29) and (40) also hold for the P_N and S_N angular discretizations (Lewis and Miller, 1993) of Eqs. (1), (2), and (5). Equations (12)–(14) with $\phi_k = 0$ for $k > N$ *are* the P_N equations, and thus the analysis in this case is nearly identical to the one presented above. [If $N = 1$, then $\phi_2 = 0$ and there is no need to develop Eq. (32)]. For the S_N discretization, the only restriction on the angular quadrature is that it integrate the first three Legendre polynomials exactly.

3. Moment Analysis of Angular Approximation Methods

We now determine the flux-weighted averages of x and $(x - x_a)^2$ corresponding to several angular approximation methods. These methods all replace Eq. (1) with an equation or set of equations for the scalar flux and possibly higher-order angular moments of

the angular flux. Similar to Eqs. (9)–(11), we define

$$\phi_m(t) = \int_{-\infty}^{\infty} x^m \phi(x, t)\, dx, \tag{41}$$

and express Eqs. (6) and (7) as

$$\langle x \rangle_\phi(t) = \frac{\phi_1(t)}{\phi_0(t)}, \tag{42}$$

and

$$\left\langle (x - x_a)^2 \right\rangle_\phi(t) = \frac{\phi_2(t) - 2x_a\phi_1(t) + x_a^2\phi_0(t)}{\phi_0(t)}. \tag{43}$$

3.1. Diffusion Approximation

The diffusion approximation of Eqs. (1), (2), and (5) is

$$\frac{1}{v}\frac{\partial \phi}{\partial t} - \frac{1}{3\Sigma_t}\frac{\partial^2 \phi}{\partial x^2} + \Sigma_a \phi = 0, \tag{44}$$

$$\lim_{|x| \to \infty} \phi = 0, \tag{45}$$

and

$$\phi(x, 0) = \Phi(x). \tag{46}$$

Multiplying Eqs. (44) and (46) by x^m, where $m \geq 0$, integrating over space, and applying Eqs. (16), (41), and (45) yields

$$\frac{1}{v}\frac{d}{dt}\phi_m - \frac{m(m-1)}{3\Sigma_t}\phi_{m-2} + \Sigma_a \phi_m = 0, \tag{47}$$

and

$$\phi_m(0) = \Phi_m. \tag{48}$$

For $m = 0$, we obtain from Eqs. (47) and (48)

$$\frac{1}{v}\frac{d}{dt}\phi_0 + \Sigma_a\phi_0 = 0, \tag{49}$$

and

$$\phi_0(0) = \Phi_0. \tag{50}$$

The solution to these two expressions is

$$\phi_0(t) = \Phi_0 e^{-\Sigma_a vt}. \tag{51}$$

For $m = 1$, Eqs. (47) and (48) become

$$\frac{1}{v}\frac{d}{dt}\phi_1 + \Sigma_a\phi_1 = 0, \tag{52}$$

and

$$\phi_1(0) = \Phi_1. \tag{53}$$

Solving Eqs. (52) and (53) gives

$$\phi_1(t) = \Phi_1 e^{-\Sigma_a vt}. \tag{54}$$

For $m = 2$, using Eqs. (47), (48), and (51) allows us to write

$$\frac{1}{v}\frac{d}{dt}\phi_2 + \Sigma_a\phi_2 = \frac{2\Phi_0}{3\Sigma_t} e^{-\Sigma_a vt}, \tag{55}$$

and

$$\phi_2(0) = \Phi_2. \tag{56}$$

When we solve Eqs. (55) and (56), we have

$$\phi_2(t) = \Phi_2 e^{-\Sigma_a vt} + \frac{2\Phi_0 vt}{3\Sigma_t} e^{-\Sigma_a vt}. \tag{57}$$

Evaluating Eqs. (42) and (43) with Eqs. (28), (39), (51), (54), and (57) shows that for the diffusion approximation

$$\langle x\rangle_{\phi}(t) = \langle x\rangle_{\Phi}, \tag{58}$$

and

$$\langle (x - x_a)^2\rangle_{\phi}(t) = \left\langle (x - x_a)^2\right\rangle_{\Phi} + \frac{2vt}{3\Sigma_{\mathrm{t}}}. \tag{59}$$

By comparing Eqs. (58) and (59) to Eqs. (29) and (40), we see that the diffusion approximation produces the correct flux-weighted average of x but not the correct flux-weighted average of $(x-x_a)^2$. This result is in contrast to steady-state radiation transport, where the diffusion approximation preserves both quantities exactly (Brantley and Larsen, 2000).

3.2. $P_{1/3}$ Approximation

Olson et al. (2000) have suggested the following modification to the P_1 equations, i.e., Eqs. (12)–(14) with $\phi_k = 0$ for $k > 1$,

$$\frac{1}{v}\frac{\partial \phi}{\partial t} + \frac{\partial J}{\partial x} + \Sigma_{\mathrm{a}}\phi = 0, \tag{60}$$

$$\frac{\eta}{v}\frac{\partial J}{\partial t} + \frac{1}{3}\frac{\partial \phi}{\partial x} + \Sigma_{\mathrm{t}} J = 0, \tag{61}$$

$$\lim_{|x|\to\infty} \phi = 0, \tag{62}$$

$$\lim_{|x|\to\infty} J = 0, \tag{63}$$

$$\phi(x, 0) = \Phi(x), \tag{64}$$

and

$$J(x, 0) = 0. \tag{65}$$

Here, $J(x, t)$ is the current,

$$J(x, t) = \int_{-1}^{1} \mu\psi(x, \mu, t)\, dx, \tag{66}$$

which, because $P_1(\mu) = \mu$, is Eq. (8) for $k = 1$. The only difference between Eqs. (60)–(65) and the P_1 equations is the coefficient η multiplying the time derivative in Eq. (61). When $\eta = 1$ we of course recover the P_1 equations, while $\eta = 0$ yields the diffusion approximation in Eqs. (44)–(46). However, setting $\eta = 1/3$ gives the $P_{1/3}$ approximation of Eqs. (1), (2), and (5), which produces solutions that propagate at the correct speed v instead of the erroneous $v/\sqrt{3}$ for P_1 (Olson et al., 2000).

To determine the flux-weighted averages of x and $(x - x_a)^2$ for the $P_{1/3}$ approximation, we first define spatial moments of the current corresponding to Eq. (41),

$$J_m(t) = \int_{-\infty}^{\infty} x^m J(x, t)\, dx. \tag{67}$$

Then, when we multiply Eqs. (60), (61), (64), and (65) by x^m, where $m \geq 0$, integrate over space, and employ Eqs. (16), (41), (62), (63), and (67), we have

$$\frac{1}{v}\frac{d}{dt}\phi_m - mJ_{m-1} + \Sigma_a\phi_m = 0, \tag{68}$$

$$\frac{\eta}{v}\frac{d}{dt}J_m - \frac{m}{3}\phi_{m-1} + \Sigma_t J_m = 0, \tag{69}$$

$$\phi_m(0) = \Phi_m, \tag{70}$$

and

$$J_m(0) = 0. \tag{71}$$

For $m = 0$, Eqs. (69)–(71) are

$$\frac{1}{v}\frac{d}{dt}\phi_0 + \Sigma_a\phi_0 = 0, \tag{72}$$

$$\frac{\eta}{v}\frac{d}{dt}J_0 + \Sigma_t J_0 = 0, \tag{73}$$

$$\phi_0(0) = \Phi_0, \tag{74}$$

and

$$J_0(0) = 0. \tag{75}$$

The solution to Eqs. (72)–(75) is

$$\phi_0(t) = \Phi_0 e^{-\Sigma_a vt}, \tag{76}$$

and

$$J_0(t) = 0. \tag{77}$$

For $m = 1$, we obtain from Eqs. (68)–(71), (76), and (77)

$$\frac{1}{v}\frac{d}{dt}\phi_1 + \Sigma_a\phi_1 = 0, \tag{78}$$

$$\frac{\eta}{v}\frac{d}{dt}J_1 + \Sigma_t J_1 = \frac{\Phi_0}{3}e^{-\Sigma_a vt}, \tag{79}$$

$$\phi_1(0) = \Phi_1, \tag{80}$$

and

$$J_1(0) = 0. \tag{81}$$

Solving these expressions yields

$$\phi_1(t) = \Phi_1 e^{-\Sigma_a vt}, \tag{82}$$

and

$$J_1(t) = \frac{\Phi_0}{3(\Sigma_t - \eta\Sigma_a)}\left(e^{-\Sigma_a vt} - e^{-\Sigma_t vt/\eta}\right). \tag{83}$$

For $m = 2$, combining Eqs. (68), (70), and (83) shows that

$$\frac{1}{v}\frac{d}{dt}\phi_2 + \Sigma_a\phi_2 = \frac{2\Phi_0}{3(\Sigma_t - \eta\Sigma_a)}\left(e^{-\Sigma_a vt} - e^{-\Sigma_t vt/\eta}\right), \tag{84}$$

and

$$\phi_2(0) = \Phi_2. \tag{85}$$

We can solve Eqs. (84) and (85) to write

$$\phi_2(t) = \Phi_2 e^{-\Sigma_a vt} + \frac{2\Phi_0}{3(\Sigma_t - \eta\Sigma_a)^2}\left\{[(\Sigma_t - \eta\Sigma_a)vt - \eta]e^{-\Sigma_a vt} + \eta e^{-\Sigma_t vt/\eta}\right\}. \tag{86}$$

Substituting Eqs. (28), (39), (76), (82), and (86) into Eqs. (42) and (43) gives

$$\langle x\rangle_\phi(t) = \langle x\rangle_\Phi, \tag{87}$$

and

$$\langle (x - x_a)^2\rangle_\phi(t) = \langle (x - x_a)^2\rangle_\Phi + \frac{2}{3(\Sigma_t - \eta\Sigma_a)^2}\{(\Sigma_t - \eta\Sigma_a)vt - \eta[1 - e^{-(\Sigma_t - \eta\Sigma_a)vt/\eta}]\}. \tag{88}$$

Equations (29) and (87) are identical, and thus the $P_{1/3}$ approximation yields the correct flux-weighted average of x. In fact, this result holds regardless of the value of η in Eq. (61). However, Eq. (88) only matches Eq. (40) if $\eta = 1$, the value for P_1. Olson (2009) has extended the idea behind the $P_{1/3}$ approximation to higher-order P_N discretizations, multiplying the time derivatives in the additional equations by coefficients chosen to preserve the correct particle speed. Our conclusions above hold in this case, as well; any choice of coefficients produces the correct flux-weighted average of x, but the coefficient multiplying the time derivative of the current must be set to unity in order to generate the correct flux-weighted average of $(x - x_a)^2$.

3.3. SP_2 *Approximation*

The SP_2 approximation of Eqs. (1) and (2) is (Frank et al., 2007)

$$\frac{1}{v}\frac{\partial \phi}{\partial t} + \Sigma_a \phi - \Sigma_t \xi = 0, \tag{89}$$

$$\frac{1}{v}\frac{\partial \xi}{\partial t} - \frac{1}{3\Sigma_t}\frac{\partial^2 \phi}{\partial x^2} - \frac{4}{15\Sigma_t}\frac{\partial^2 \xi}{\partial x^2} + \Sigma_t \xi = 0, \tag{90}$$

$$\lim_{|x|\to\infty} \phi = 0, \tag{91}$$

and

$$\lim_{|x|\to\infty} \xi = 0. \tag{92}$$

In these expressions, $\xi(x, t)$ is an auxiliary variable. Also, corresponding to Eq. (5), the initial condition for ϕ is

$$\phi(x, 0) = \Phi(x), \tag{93}$$

while the initial condition for ξ satisfies

$$-\frac{4}{15\Sigma_t}\frac{d^2}{dx^2}\xi(x, 0) + \Sigma_t \xi(x, 0) = \frac{1}{3\Sigma_t}\frac{d^2 \Phi}{dx^2}, \tag{94}$$

which is a steady-state version of Eq. (90) evaluated at $t = 0$ with Eq. (93). Similar to Eq. (41), we define

$$\xi_m(t) = \int_{-\infty}^{\infty} x^m \xi(x, t)\, dx. \tag{95}$$

Then, multiplying Eqs. (89), (90), (93), and (94) by x^m, where $m \geq 0$, integrating over space, and making use of Eqs. (16), (41), (91), (92), and (95) allows us to write

$$\frac{1}{v}\frac{d}{dt}\phi_m + \Sigma_a \phi_m - \Sigma_t \xi_m = 0, \tag{96}$$

$$\frac{1}{v}\frac{d}{dt}\xi_m - \frac{m(m-1)}{3\Sigma_t}\phi_{m-2} - \frac{4m(m-1)}{15\Sigma_t}\xi_{m-2} + \Sigma_t \xi_m = 0, \tag{97}$$

$$\phi_m(0) = \Phi_m, \tag{98}$$

and

$$-\frac{4m(m-1)}{15\Sigma_t}\xi_{m-2}(0)+\Sigma_t\xi_m(0)=\frac{m(m-1)}{3\Sigma_t}\Phi_{m-2}. \tag{99}$$

For $m=0$, Eqs. (96)–(99) become

$$\frac{1}{v}\frac{d}{dt}\phi_0+\Sigma_a\phi_0-\Sigma_t\xi_0=0, \tag{100}$$

$$\frac{1}{v}\frac{d}{dt}\xi_0+\Sigma_t\xi_0=0, \tag{101}$$

$$\phi_0(0)=\Phi_0, \tag{102}$$

and

$$\xi_0(0)=0. \tag{103}$$

Solving Eqs. (101)–(103) gives

$$\phi_0(t)=\Phi_0 e^{-\Sigma_a vt}, \tag{104}$$

and

$$\xi_0(t)=0. \tag{105}$$

For $m=1$, Eqs. (96)–(99) yield

$$\frac{1}{v}\frac{d}{dt}\phi_1+\Sigma_a\phi_1-\Sigma_t\xi_1=0, \tag{106}$$

$$\frac{1}{v}\frac{d}{dt}\xi_1+\Sigma_t\xi_1=0, \tag{107}$$

$$\phi_1(0)=\Phi_1, \tag{108}$$

and

$$\xi_1(0)=0. \tag{109}$$

The solution to Eqs. (106)–(109) is

$$\phi_1(t)=\Phi_1 e^{-\Sigma_a vt}, \tag{110}$$

and

$$\xi_1(t) = 0. \tag{111}$$

For $m = 2$, we obtain from Eqs. (96)–(99), (104), and (105)

$$\frac{1}{v}\frac{d}{dt}\phi_2 + \Sigma_a\phi_2 - \Sigma_t\xi_2 = 0, \tag{112}$$

$$\frac{1}{v}\frac{d}{dt}\xi_2 + \Sigma_t\xi_2 = \frac{2\Phi_0}{3\Sigma_t}e^{-\Sigma_a vt}, \tag{113}$$

$$\phi_2(0) = \Phi_2, \tag{114}$$

and

$$\xi_2(0) = \frac{2\Phi_0}{3\Sigma_t^2}. \tag{115}$$

By solving Eqs. (112)–(115), we see that

$$\phi_2(t) = \Phi_2 e^{-\Sigma_a vt} + \frac{2\Phi_0}{3\Sigma_t\Sigma_s^2}\left[(\Sigma_t\Sigma_s vt - \Sigma_a)e^{-\Sigma_a vt} + \Sigma_a e^{-\Sigma_t vt}\right], \tag{116}$$

and

$$\xi_2(t) = \frac{2\Phi_0}{3\Sigma_t^2\Sigma_s}\left(\Sigma_t e^{-\Sigma_a vt} - \Sigma_a e^{-\Sigma_t vt}\right). \tag{117}$$

When we evaluate Eqs. (42) and (43) with Eqs. (28), (39), (104), (110), and (116), we have

$$\langle x\rangle_\phi(t) = \langle x\rangle_\Phi, \tag{118}$$

and

$$\langle (x - x_a)^2\rangle_\phi(t) = \langle (x - x_a)^2\rangle_\Phi + \frac{2}{3\Sigma_t\Sigma_s^2}\left[\Sigma_t\Sigma_s vt - \Sigma_a\left(1 - e^{-\Sigma_s vt}\right)\right]. \tag{119}$$

A comparison of Eqs. (29), (40), (118), and (119) reveals that, as with the diffusion and $P_{1/3}$ approximations, the SP_2 approximation preserves the correct flux-weighted average of x but not the correct flux-weighted average of $(x - x_a)^2$.

3.4. SP_3 Approximation

The SP_3 approximation of Eqs. (1) and (2) is (Frank et al., 2007)

$$\frac{1}{v}\frac{\partial \phi}{\partial t} - \frac{1}{3\Sigma_t}\frac{\partial^2 \phi}{\partial x^2} - \frac{2}{3\Sigma_t}\frac{\partial^2 \chi}{\partial x^2} + \frac{1}{3\Sigma_t}\frac{\partial^2 \zeta}{\partial x^2} + \Sigma_a \phi = 0, \quad (120)$$

$$\frac{\alpha}{v}\frac{\partial \chi}{\partial t} - \frac{2}{45\Sigma_t}\frac{\partial^2 \phi}{\partial x^2} - \frac{11}{63\Sigma_t}\frac{\partial^2 \chi}{\partial x^2} + \frac{\Sigma_t}{3}\chi = 0, \quad (121)$$

$$\frac{1}{v}\frac{\partial \zeta}{\partial t} - \frac{1}{3\Sigma_t}\frac{\partial^2 \phi}{\partial x^2} - \frac{2}{3\Sigma_t}\frac{\partial^2 \chi}{\partial x^2} - \frac{12(1-\alpha) - 5}{15\Sigma_t}\frac{\partial^2 \zeta}{\partial x^2} + \Sigma_a \phi + \Sigma_t \zeta = 0, \quad (122)$$

$$\lim_{|x|\to\infty} \phi = 0, \quad (123)$$

$$\lim_{|x|\to\infty} \chi = 0, \quad (124)$$

and

$$\lim_{|x|\to\infty} \zeta = 0. \quad (125)$$

Here, $\chi(x, t)$ and $\zeta(x, t)$ are auxiliary variables and $0 \le \alpha \le 1$ is an adjustable parameter that controls robustness. Note that when $\alpha = 0$ the time derivative in Eq. (121) vanishes, whereas $\alpha \gtrsim 0.9$ results in an ill-posed system of equations (Frank et al., 2007). In addition, the initial condition for ϕ that replaces Eq. (5) is

$$\phi(x, 0) = \Phi(x), \quad (126)$$

while the initial condition for ζ is given by

$$\zeta(x, 0) = 0. \quad (127)$$

Frank et al. (2007) also propose two different initial conditions for χ. The first is described by a steady-state version of Eq. (121)

evaluated at $t = 0$ using Eq. (126), similar to Eq. (94),

$$-\frac{11}{63\Sigma_t}\frac{d^2}{dx^2}\chi(x,0) + \frac{\Sigma_t}{3}\chi(x,0) = \frac{2}{45\Sigma_t}\frac{d^2\Phi}{dx^2}. \tag{128}$$

The second follows from identifying χ as the second Legendre moment of the angular flux, i.e., Eq. (8) for $k = 2$. Substituting Eq. (5) into this expression yields

$$\chi(x,0) = 0. \tag{129}$$

If we define spatial moments of χ and ζ corresponding to Eq. (41),

$$\chi_m(t) = \int_{-\infty}^{\infty} x^m \chi(x,t)\,dx, \tag{130}$$

and

$$\zeta_m(t) = \int_{-\infty}^{\infty} x^m \zeta(x,t)\,dx, \tag{131}$$

then we can multiply Eqs. (120)–(122) and (126)–(129) by x^m, where $m \geq 0$, integrate over space, and apply Eqs. (16), (41), (123)–(125), (130), and (131) to show that

$$\frac{1}{v}\frac{d}{dt}\phi_m - \frac{m(m-1)}{3\Sigma_t}\phi_{m-2} - \frac{2m(m-1)}{3\Sigma_t}\chi_{m-2} + \frac{m(m-1)}{3\Sigma_t}\zeta_{m-2} + \Sigma_a\phi_m = 0, \tag{132}$$

$$\frac{\alpha}{v}\frac{d}{dt}\chi_m - \frac{2m(m-1)}{45\Sigma_t}\phi_{m-2} - \frac{11m(m-1)}{63\Sigma_t}\chi_{m-2} + \frac{\Sigma_t}{3}\chi_m = 0, \tag{133}$$

$$\frac{1}{v}\frac{d}{dt}\zeta_m - \frac{m(m-1)}{3\Sigma_t}\phi_{m-2} - \frac{2m(m-1)}{3\Sigma_t}\chi_{m-2} - \frac{[12(1-\alpha)-5]m(m-1)}{15\Sigma_t}\zeta_{m-2} + \Sigma_a\phi_m + \Sigma_t\zeta_m = 0, \tag{134}$$

$$\phi_m(0) = \Phi_m, \tag{135}$$

$$\zeta_m(0) = 0, \tag{136}$$

and

$$-\frac{11m(m-1)}{63\Sigma_t}\chi_{m-2}(0) + \frac{\Sigma_t}{3}\chi_m(0) = \frac{2m(m-1)}{45\Sigma_t}\Phi_{m-2}, \tag{137}$$

or

$$\chi_m(0) = 0. \tag{138}$$

For $m = 0$, Eqs. (132)–(136) are

$$\frac{1}{v}\frac{d}{dt}\phi_0 + \Sigma_a\phi_0 = 0, \tag{139}$$

$$\frac{\alpha}{v}\frac{d}{dt}\chi_0 + \frac{\Sigma_t}{3}\chi_0 = 0, \tag{140}$$

$$\frac{1}{v}\frac{d}{dt}\zeta_0 + \Sigma_a\phi_0 + \Sigma_t\zeta_0 = 0, \tag{141}$$

$$\phi_0(0) = \Phi_0, \tag{142}$$

and

$$\zeta_0(0) = 0, \tag{143}$$

while Eqs. (137) and (138) both become

$$\chi_0(0) = 0. \tag{144}$$

When we solve Eqs. (139)–(144), we have

$$\phi_0(t) = \Phi_0 e^{-\Sigma_a vt}, \tag{145}$$

$$\chi_0(t) = 0, \tag{146}$$

and

$$\zeta_0(t) = -\frac{\Sigma_a\Phi_0}{\Sigma_s}\left(e^{-\Sigma_a vt} - e^{-\Sigma_t vt}\right). \tag{147}$$

For $m = 1$, we obtain from Eqs. (132) and (135)

$$\frac{1}{v}\frac{d}{dt}\phi_1 + \Sigma_a\phi_1 = 0, \tag{148}$$

and

$$\phi_1(0) = \Phi_1. \tag{149}$$

Solving Eqs. (148) and (149) gives

$$\phi_1(t) = \Phi_1 e^{-\Sigma_a vt}. \tag{150}$$

For $m = 2$, combining Eqs. (132), (135), and (145)–(147) allows us to write

$$\frac{1}{v}\frac{d}{dt}\phi_2 + \Sigma_a\phi_2 = \frac{2\Phi_0}{3\Sigma_t\Sigma_s}\left(\Sigma_t e^{-\Sigma_a vt} - \Sigma_a e^{-\Sigma_t vt}\right), \tag{151}$$

and

$$\phi_2(0) = \Phi_2. \tag{152}$$

The solution to these two expressions is

$$\phi_2(t) = \Phi_2 e^{-\Sigma_a vt} + \frac{2\Phi_0}{3\Sigma_t\Sigma_s^2}\left[(\Sigma_t\Sigma_s vt - \Sigma_a)\, e^{-\Sigma_a vt} + \Sigma_a e^{-\Sigma_t vt}\right]. \tag{153}$$

Equations (145), (150), and (153) are the same as Eqs. (104), (110), and (116), and thus Eqs. (42) and (43) are identical between the SP_2 and SP_3 approximations. This result does not depend on the value of α or which initial condition for χ is used.

3.5. SSP$_3$ *Approximation*

Frank et al. (2007) have suggested simplifying the SP_3 approximation and also improving its robustness by neglecting ζ. Equations (120)–(129) then reduce to the SSP_3 approximation of Eqs. (1),

(2), and (5),

$$\frac{1}{v}\frac{\partial\phi}{\partial t} - \frac{1}{3\Sigma_t}\frac{\partial^2\phi}{\partial x^2} - \frac{2}{3\Sigma_t}\frac{\partial^2\chi}{\partial x^2} + \Sigma_a\phi = 0, \tag{154}$$

$$\frac{\alpha}{v}\frac{\partial\chi}{\partial t} - \frac{2}{45\Sigma_t}\frac{\partial^2\phi}{\partial x^2} - \frac{11}{63\Sigma_t}\frac{\partial^2\chi}{\partial x^2} + \frac{\Sigma_t}{3}\chi = 0, \tag{155}$$

$$\lim_{|x|\to\infty}\phi = 0, \tag{156}$$

$$\lim_{|x|\to\infty}\chi = 0, \tag{157}$$

$$\phi(x,0) = \Phi(x), \tag{158}$$

and

$$-\frac{11}{63\Sigma_t}\frac{d^2}{dx^2}\chi(x,0) + \frac{\Sigma_t}{3}\chi(x,0) = \frac{2}{45\Sigma_t}\frac{d^2\Phi}{dx^2}, \tag{159}$$

or

$$\chi(x,0) = 0. \tag{160}$$

In addition, we immediately obtain from Eqs. (132)–(138)

$$\frac{1}{v}\frac{d}{dt}\phi_m - \frac{m(m-1)}{3\Sigma_t}\phi_{m-2} - \frac{2m(m-1)}{3\Sigma_t}\chi_{m-2} + \Sigma_a\phi_m = 0, \tag{161}$$

$$\frac{\alpha}{v}\frac{d}{dt}\chi_m - \frac{2m(m-1)}{45\Sigma_t}\phi_{m-2} - \frac{11m(m-1)}{63\Sigma_t}\chi_{m-2} + \frac{\Sigma_t}{3}\chi_m = 0, \tag{162}$$

$$\phi_m(0) = \Phi_m, \tag{163}$$

and

$$-\frac{11m(m-1)}{63\Sigma_t}\chi_{m-2}(0) + \frac{\Sigma_t}{3}\chi_m(0) = \frac{2m(m-1)}{45\Sigma_t}\Phi_{m-2}, \tag{164}$$

or

$$\chi_m(0) = 0. \tag{165}$$

For $m = 0$, Eqs. (161)–(163) become

$$\frac{1}{v}\frac{d}{dt}\phi_0 + \Sigma_a\phi_0 = 0, \tag{166}$$

$$\frac{\alpha}{v}\frac{d}{dt}\chi_0 + \frac{\Sigma_t}{3}\chi_0 = 0, \tag{167}$$

and

$$\phi_0(0) = \Phi_0, \tag{168}$$

and Eqs. (164) and (165) both yield

$$\chi_0(0) = 0. \tag{169}$$

Solving Eqs. (166)–(169) gives

$$\phi_0(t) = \Phi_0 e^{-\Sigma_a vt}, \tag{170}$$

and

$$\chi_0(t) = 0. \tag{171}$$

For $m = 1$, Eqs. (161) and (163) are

$$\frac{1}{v}\frac{d}{dt}\phi_1 + \Sigma_a\phi_1 = 0, \tag{172}$$

and

$$\phi_1(0) = \Phi_1. \tag{173}$$

The solution to Eqs. (172) and (173) is

$$\phi_1(t) = \Phi_1 e^{-\Sigma_a vt}. \tag{174}$$

For $m = 2$, Eqs. (161), (163), (170), and (171) show that

$$\frac{1}{v}\frac{d}{dt}\phi_2 + \Sigma_a\phi_2 = \frac{2\Phi_0}{3\Sigma_t}e^{-\Sigma_a vt}, \tag{175}$$

and

$$\phi_2(0) = \Phi_2. \tag{176}$$

When we solve Eqs. (175) and (176), we have

$$\phi_2(t) = \Phi_2 e^{-\Sigma_a vt} + \frac{2\Phi_0 vt}{3\Sigma_t}e^{-\Sigma_a vt}. \tag{177}$$

Equations (170), (174), and (177) are identical to Eqs. (51), (54), and (57), which results in Eqs. (42) and (43) being the same for the SSP_3 approximation as the diffusion approximation. Again, this outcome holds regardless of the value of α or the choice of initial condition for χ.

4. Comparison of Moment Errors

We found in the previous section that all of the angular approximation methods we consider preserve the correct flux-weighted average of x but generate an incorrect flux-weighted average of $(x - x_a)^2$. To examine the errors in this latter quantity, we express the flux-weighted average of $(x - x_a)^2$ corresponding to each method as the exact result given by Eq. (40) plus a time-dependent error term $E(t)$,

$$\langle (x - x_a)^2\rangle_\phi(t) = \langle (x - x_a)^2\rangle_\Phi + \frac{2}{3\Sigma_s^2}(\Sigma_s vt - 1 + e^{-\Sigma_s vt}) + E(t). \tag{178}$$

Comparing Eq. (178) to Eqs. (59), (88), and (119) shows that for the diffusion and SSP_3 approximations

$$E(t) = \frac{2}{3\Sigma_t\Sigma_s^2}[-\Sigma_s\Sigma_a vt + \Sigma_t(1 - e^{-\Sigma_s vt})], \tag{179}$$

for the $P_{1/3}$ approximation

$$E(t) = \frac{2}{3(\Sigma_t - \eta\Sigma_a)^2\Sigma_s^2}\Big\{ -(1-\eta)(\Sigma_t - \eta\Sigma_a)\Sigma_s\Sigma_a vt - \eta\Sigma_s^2[1 - e^{-(\Sigma_t - \eta\Sigma_a)vt/\eta}] + (\Sigma_t - \eta\Sigma_a)^2(1 - e^{-\Sigma_s vt})\Big\}, \tag{180}$$

and for the SP_2 and SP_3 approximations

$$E(t) = \frac{2}{3\Sigma_t\Sigma_s}(1 - e^{-\Sigma_s vt}). \tag{181}$$

Equations (179)–(181) have a complicated dependence on not only the elapsed time but also the cross sections, and thus a general comparison of these expressions is difficult. However, a limit of interest is the behavior of these error terms for large t and arbitrary cross sections. In this case, Eqs. (179)–(181) become for the diffusion and SSP_3 approximations

$$E(t) \sim -\frac{2\Sigma_a vt}{3\Sigma_t\Sigma_s}, \tag{182}$$

for the $P_{1/3}$ approximation

$$E(t) \sim -\frac{2(1-\eta)\Sigma_a vt}{3(\Sigma_t - \eta\Sigma_a)\Sigma_s}, \tag{183}$$

and for the SP_2 and SP_3 approximations

$$E(t) \sim \frac{2}{3\Sigma_t\Sigma_s}. \tag{184}$$

From Eq. (182) we see that the diffusion and SSP_3 error is negative for large t, implying that the flux-weighted average of $(x - x_a)^2$ is too small. This result is somewhat counterintuitive, as it is well known that the diffusion approximation produces solutions that propagate too quickly, a deficiency that should cause the flux-weighted average of $(x - x_a)^2$ to be too large. Of course, the explanation of this contradiction is that solutions generated by the

diffusion approximation are also attenuated too much. Equation (183) shows that the $P_{1/3}$ error is also negative for large t. Simmons and Mihalas (2000) have demonstrated through a perturbation analysis of the $P_{1/3}$ approximation that this method can also attenuate solutions too much, which is consistent with Eq. (183). By comparing Eqs. (182) and (183), we additionally see that the $P_{1/3}$ error is smaller in magnitude than the diffusion and SSP_3 error for large t. However, the angular approximation methods with the smallest error in magnitude for large t are the SP_2 and SP_3 approximations, as seen from Eq. (184). Clearly, this error term is bounded independently of the elapsed time, unlike Eqs. (182) and (183). Thus, we expect the SP_2 and SP_3 approximations to be more accurate than the diffusion, $P_{1/3}$, and SSP_3 approximations for sufficiently large elapsed times.

5. Improved SP_2 Approximation

In the SP_3 and SSP_3 approximations, there are two different initial conditions for the auxiliary variable χ. The first initial condition satisfies a time-independent equation given by Eq. (128) or (159), while the second initial condition is developed by identifying χ as the second Legendre moment of the angular flux and in our case is zero, as in Eq. (129) or (160). However, for the SP_2 approximation we only have one initial condition for the auxiliary variable ξ, which is defined by Eq. (94). An alternative to solving this time-independent equation is to set the initial value of ξ equal to zero, too, i.e.,

$$\xi(x, 0) = 0. \tag{185}$$

Not only does this initial condition simplify the SP_2 approximation, it should also improve the accuracy of this method, as we will see shortly.

When Eq. (185) replaces Eq. (94), Eqs. (104), (105), (110), (111), and therefore Eq. (118) remain unchanged, whereas Eq. (115) becomes

$$\xi_2(0) = 0. \tag{186}$$

Using this expression along with Eq. (114) as the initial conditions for Eqs. (112) and (113) shows that Eqs. (116) and (117) are now

$$\phi_2(t) = \Phi_2 e^{-\Sigma_a vt} + \frac{2\Phi_0}{3\Sigma_s^2}[(\Sigma_s vt - 1)e^{-\Sigma_a vt} + e^{-\Sigma_t vt}], \quad (187)$$

and

$$\xi_2(t) = \frac{2\Phi_0}{3\Sigma_t\Sigma_s}(e^{-\Sigma_a vt} - e^{-\Sigma_t vt}), \quad (188)$$

respectively. We can then substitute Eqs. (39), (104), (110), and (187) into Eq. (43) to write

$$\langle (x - x_a)^2 \rangle_\phi(t) = \langle (x - x_a)^2 \rangle_\Phi + \frac{2}{3\Sigma_s^2}(\Sigma_s vt - 1 + e^{-\Sigma_s vt}). \quad (189)$$

Equations (40) and (189) are identical, and thus employing Eq. (186) as the initial condition for ξ in the SP_2 approximation preserves the correct flux-weighted average of $(x - x_a)^2$. We therefore expect this improved SP_2 approximation to be more accurate than the other angular approximation methods.

6. Numerical Results

We now test our theoretical predictions regarding the error in the flux-weighted average of $(x - x_a)^2$ for each angular approximation method by calculating this quantity directly from numerical results. These results also allow us to relate the accuracy of the flux-weighted average of $(x - x_a)^2$ to the overall accuracy of the method. As we will see, an accurate value for this flux-weighted average does not necessarily guarantee an accurate solution.

We consider two problems corresponding to a nondimensional version of the Eqs. (1), (2), and (5) with $\Sigma_t = 1.0$, $\Sigma_a = 0.3$, and $v = 1$. The problems differ in their initial conditions, which are symmetric about $x = 8$. We simulated these problems using the diffusion, $P_{1/3}$, SP_2, SP_3, and SSP_3 approximations along with the improved SP_2 approximation and the P_1 discretization out to elapsed times of $t = 1$, 5, and 15. In the SP_3 and SSP_3 approximations we set $\alpha = 2/3$. For the diffusion and simplified

P_N calculations we employed a basic finite difference scheme with backward Euler time integration, while for the $P_{1/3}$ and P_1 calculations we used a semi-implicit discontinuous Galerkin method (McClarren et al., 2008). Furthermore, we performed our simulations on a sequence of uniform spatial grids with an increasing number of cells and a time-step size of $\Delta t = 0.3\Delta x$. From this sequence we computed the flux-weighted average of $(x - x_a)^2$ for $x_a = 8$ using Wynn-epsilon acceleration (Bornemann et al., 2004; Ganapol, 2008). For the different elapsed times we specified different spatial domains: $x \in [0, 16]$ for $t = 1$, $x \in [-4, 20]$ for $t = 5$, and $x \in [-10, 26]$ for $t = 15$. We also generated reference transport solutions using high-order P_N discretizations (P_{99} for $t = 1$ and P_{29} and for $t = 5$ and 15) and the semi-implicit discontinuous Galerkin method (McClarren et al., 2008).

In Figure 1 we plot the absolute value of the error in the flux-weighted average of $(x - x_a)^2$ given by Eqs. (179)–(181) as a function of vt for the cross sections specified previously. At early times, we see that the errors for all of the angular approximation methods are comparable, with the $P_{1/3}$ approximation marginally better. Later near $vt = 5$, the error for the $P_{1/3}$ approximation is nearly zero. Then at late times, the SP_2 and SP_3 approximations have the smallest error in magnitude. We therefore expect that the angular approximation method that is the most accurate to vary as a function of time.

In the numerical results that follow, we use the term "initial smoothing" with the SP_3 and SSP_3 approximations to denote that

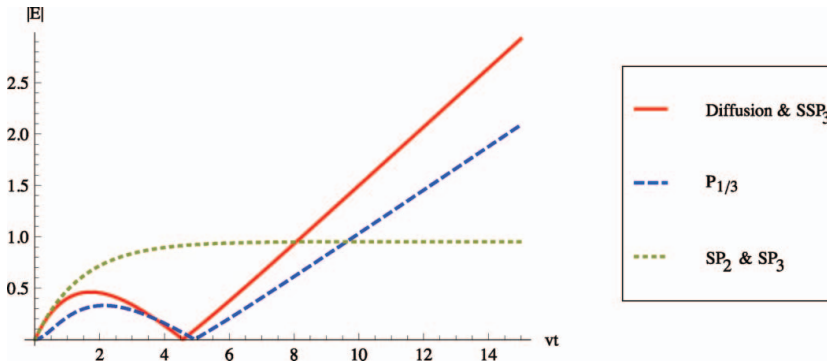

FIGURE 1 Absolute value of the error in $\langle (x - x_a)^2 \rangle_\phi$ as a function of vt.

a time-independent equation, Eq. (128) or (159), was solved to determine the initial condition for the auxiliary variable χ. When this term is absent, the alternate initial condition, Eq. (129) or (160), was applied. Also, in addition to the flux-weighted average of $(x - x_a)^2$, we report the error in the scalar flux with respect to the reference transport solution for each angular approximation method as measured by the 2-norm on the finest spatial grid. Furthermore, we plot the scalar flux for this grid and $x \geq 8$ only as the two problems are symmetric about this point.

The first problem has an initial condition consisting of a square pulse,

$$\Phi(x) = \begin{cases} 1 & 7 \leq x \leq 9 \\ 0 & \text{otherwise} \end{cases}. \tag{190}$$

We simulated this problem using spatial grids with 2^j cells, where $j = 4 \ldots 10$. The results from these simulations are given in Figures 2–4 and Tables 1–3.

In Figure 2 the scalar flux at $t = 1$ is plotted. Perhaps unsurprisingly none of the angular approximation methods captures the reference transport solution well: at such an early time the solution is dominated by free streaming, for which low-order angular discretization schemes like the approximation methods

TABLE 1 Theoretical and Numerical Values of $\langle (x - x_a)^2 \rangle_\phi$ and Error in the Scalar Flux for the First Problem at $t = 1$

Method	Theoretical $\langle (x - x_a)^2 \rangle_\phi$	Numerical $\langle (x - x_a)^2 \rangle_\phi$	$\|\|\phi_{\text{trans}} - \phi\|\|_2$
Transport	0.60080	—	—
P_1	0.60080	0.60082	0.31277
$P_{1/3}$	0.81816	0.81817	0.28555
Diffusion	1.00000	1.00000	0.27561
SP_2	1.08024	1.08017	0.31533
Improved SP_2	0.60080	0.60080	0.26538
SP_3 w/init. smoothing	1.08024	1.07913	0.27386
SP_3	1.08024	1.08024	0.28055
SSP_3 w/init. smoothing	1.00000	0.99854	0.29040
SSP_3	1.00000	1.00000	0.28021

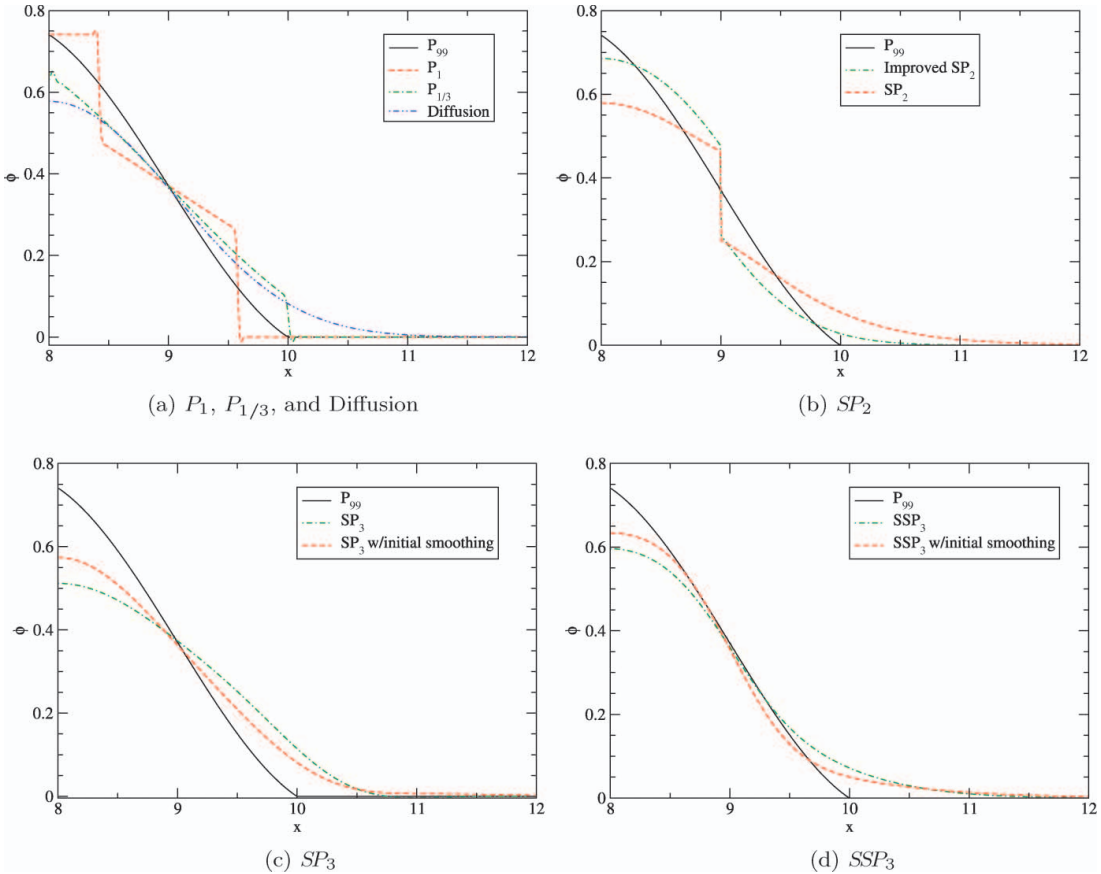

(a) P_1, $P_{1/3}$, and Diffusion (b) SP_2

(c) SP_3 (d) SSP_3

FIGURE 2 First problem scalar flux at $t = 1$.

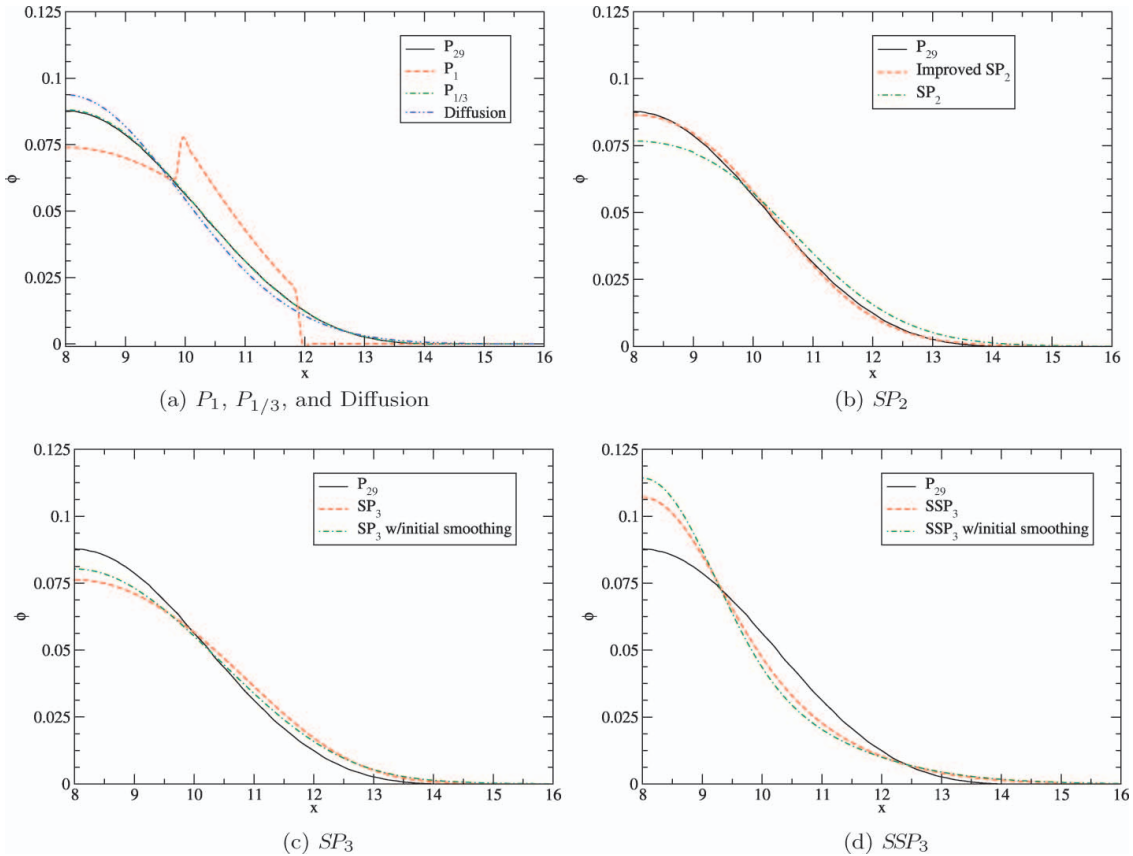

(a) P_1, $P_{1/3}$, and Diffusion (b) SP_2

(c) SP_3 (d) SSP_3

FIGURE 3 First problem scalar flux at $t = 5$.

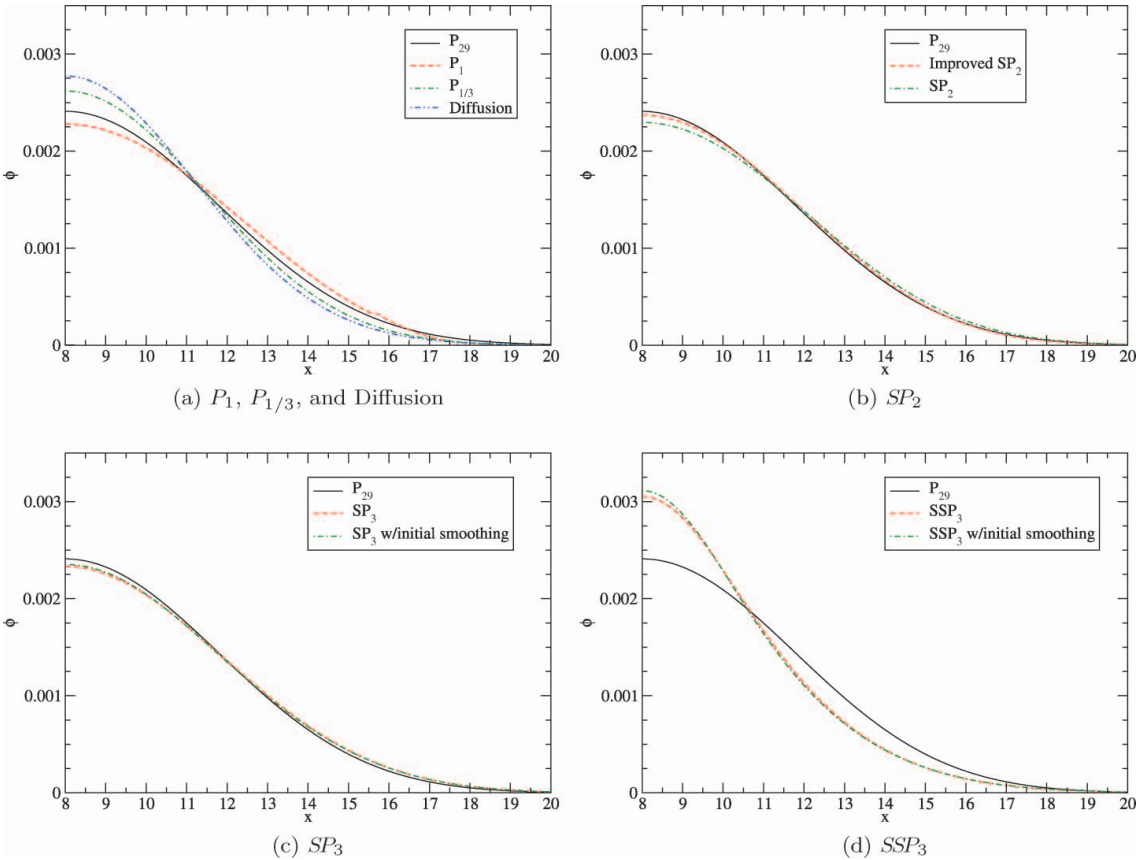

(a) P_1, $P_{1/3}$, and Diffusion

(b) SP_2

(c) SP_3

(d) SSP_3

FIGURE 4 First problem scalar flux at $t = 15$.

TABLE 2 Theoretical and Numerical Values of $\langle (x - x_a)^2 \rangle_\phi$ and Error in the Scalar Flux for the First Problem at $t = 5$

Method	Theoretical $\langle (x - x_a)^2 \rangle_\phi$	Numerical $\langle (x - x_a)^2 \rangle_\phi$	$\|\|\phi_{\text{trans}} - \phi\|\|_2 \times 10^3$
Transport	3.77578	—	—
P_1	3.77578	3.77213	6.91272
$P_{1/3}$	3.76269	3.76236	0.16214
Diffusion	3.66667	3.66662	2.02640
SP_2	4.69940	4.69979	3.33851
Improved SP_2	3.77578	3.77629	0.68197
SP_3 w/init. smoothing	4.69940	4.69959	3.33851
SP_3	4.69940	4.69993	3.88592
SSP_3 w/init. smoothing	3.66667	3.66579	7.73697
SSP_3	3.66667	3.66658	5.73906

we consider are, in general, woefully inaccurate. Indeed, Table 1 shows that at this time all the methods have about the same error.

The numerical results at $t = 5$ are displayed in Figure 3 and Table 2. Here, we see that the $P_{1/3}$ and improved SP_2 approximations have the smallest error. This observation is consistent with the corresponding values for the flux-weighted average of $(x - x_a)^2$, which are very accurate. Note also that although the flux-weighted average of $(x - x_a)^2$ for both versions of the SSP_3

TABLE 3 Theoretical and Numerical Values of $\langle (x - x_a)^2 \rangle_\phi$ and Error in the Scalar Flux for the First Problem at $t = 15$

Method	Theoretical $\langle (x - x_a)^2 \rangle_\phi$	Numerical $\langle (x - x_a)^2 \rangle_\phi$	$\|\|\phi_{\text{trans}} - \phi\|\|_2 \times 10^4$
Transport	13.2585	—	—
P_1	13.2585	13.2747	0.77078
$P_{1/3}$	11.1701	11.1847	1.09592
Diffusion	10.3333	10.3868	1.81881
SP_2	14.2109	14.2513	0.57862
Improved SP_2	13.2585	13.2990	0.19938
SP_3 w/init. smoothing	14.2109	14.2511	0.43971
SP_3	14.2109	14.2513	0.36923
SSP_3 w/init. smoothing	10.3333	10.3852	2.97479
SSP_3	10.3333	10.3858	2.77415

approximation and the P_1 discretization is close to the exact value, these methods have the highest error.

Figure 4 and Table 3 show that at $t = 15$ the SP_2 approximation, both versions of the SP_3 approximation, the improved SP_2 approximation, and the P_1 discretization have the most accurate values for the flux-weighted average of $(x - x_a)^2$, as predicted by our theory. These methods also have the smallest error in their scalar flux. In addition, we see that the accuracy of the $P_{1/3}$ approximation at $t = 5$ does not guarantee accuracy at this later time.

The second problem has an initial scalar flux characterized by a Gaussian profile,

$$\Phi(x) = e^{-4(x-8)^2}. \tag{191}$$

We simulated this problem again using spatial grids with 2^j cells, where $j = 5 \ldots 11$ in this case. The results generated by these simulations are displayed in Figures 5–7 and Tables 4–6.

Our previous comments for the first problem apply to this problem, too. At $t = 1$, Figure 5 and Table 4 show that no angular approximation method is very accurate. Later at $t = 5$, we see from Figure 6 and Table 5 that the $P_{1/3}$ and improved SP_2 approximations match the reference transport solution the best. The flux-weighted average of $(x - x_a)^2$ for these two methods is also very close to the exact value. As before, both versions of the SSP_3

TABLE 4 Theoretical and Numerical Values of $\langle (x - x_a)^2 \rangle_\phi$ and Error in the Scalar Flux for the Second Problem at $t = 1$

Method	Theoretical $\langle (x - x_a)^2 \rangle_\phi$	Numerical $\langle (x - x_a)^2 \rangle_\phi$	$\|\|\phi_{\text{trans}} - \phi\|\|_2 \times 10^2$
Transport	0.39246	—	—
P_1	0.39246	0.39091	2.5802
$P_{1/3}$	0.60983	0.60982	4.3836
Diffusion	0.79167	0.79167	3.7028
SP_2	0.87191	0.87176	3.1799
Improved SP_2	0.39246	0.39247	3.1718
SP_3 w/init. smoothing	0.87191	0.87098	4.1592
SP_3	0.87191	0.87191	6.5069
SSP_3 w/init. smoothing	0.79167	0.79044	2.0607
SSP_3	0.79167	0.79167	2.7127

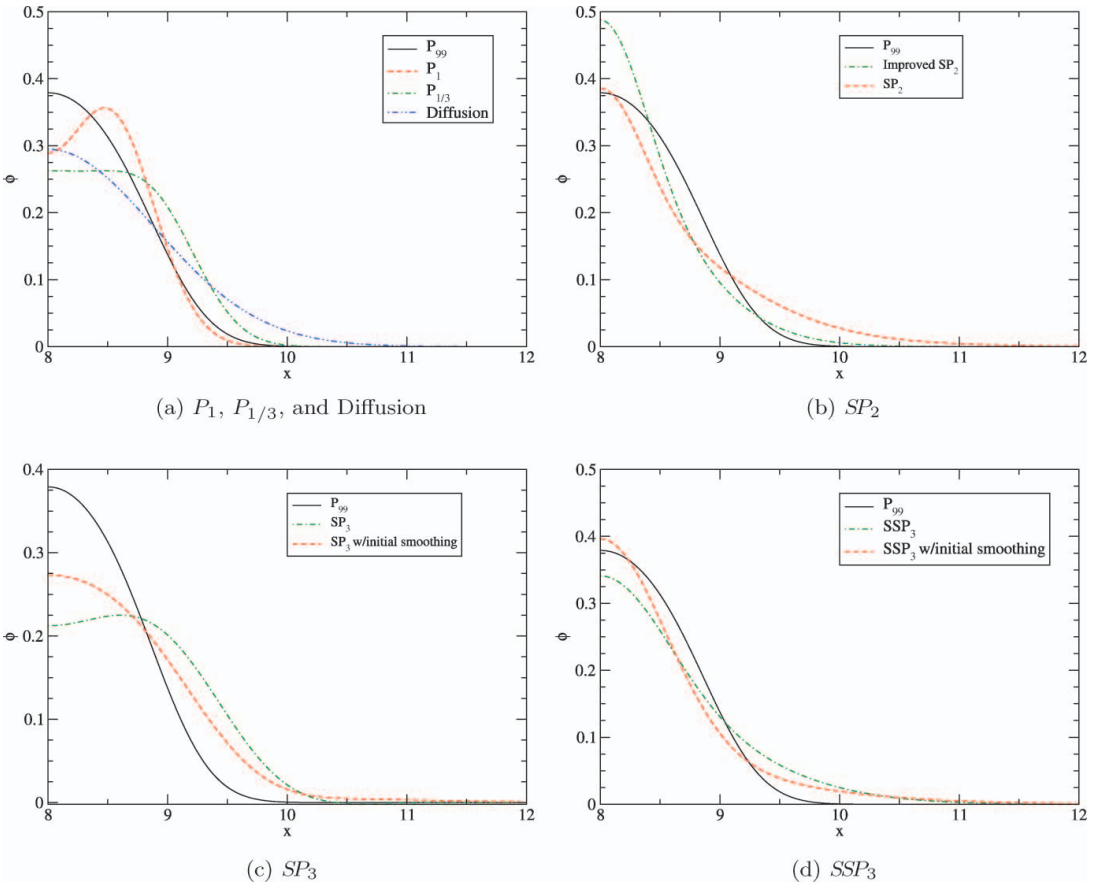

(a) P_1, $P_{1/3}$, and Diffusion

(b) SP_2

(c) SP_3

(d) SSP_3

FIGURE 5 Second problem scalar flux at $t = 1$.

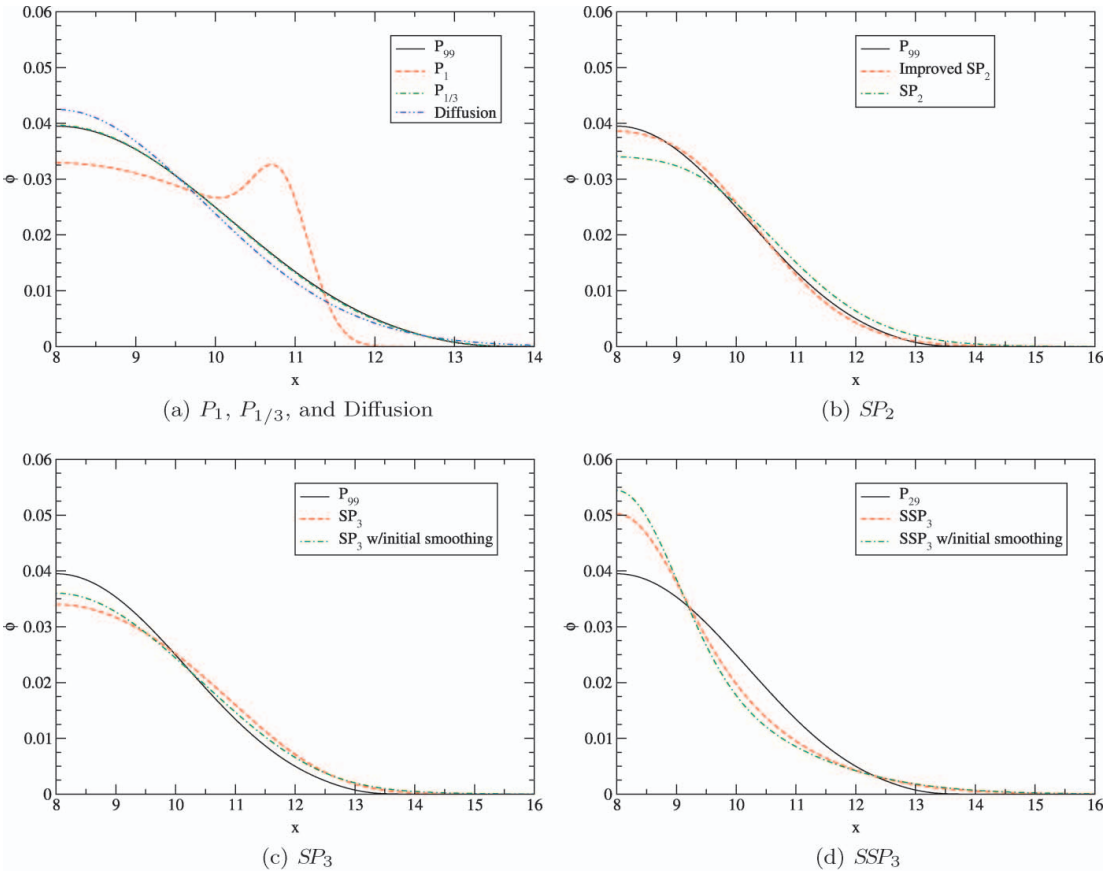

(a) P_1, $P_{1/3}$, and Diffusion (b) SP_2

(c) SP_3 (d) SSP_3

FIGURE 6 Second problem scalar flux at $t = 5$.

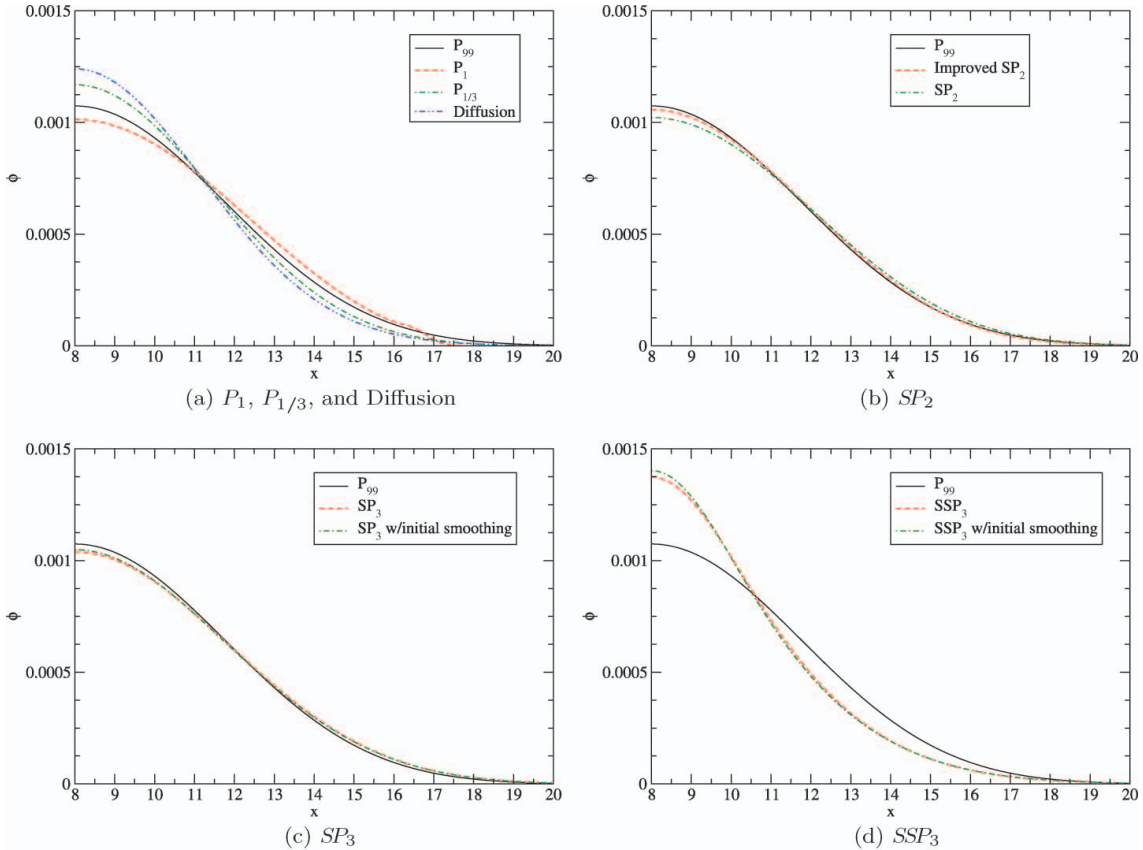

(a) P_1, $P_{1/3}$, and Diffusion

(b) SP_2

(c) SP_3

(d) SSP_3

FIGURE 7 Second problem scalar flux at $t = 15$.

TABLE 5 Theoretical and Numerical Values of $\langle (x - x_a)^2 \rangle_\phi$ and Error in the Scalar Flux for the Second Problem at $t = 5$

Method	Theoretical $\langle (x - x_a)^2 \rangle_\phi$	Numerical $\langle (x - x_a)^2 \rangle_\phi$	$\|\|\phi_{\text{trans}} - \phi\|\|_2 \times 10^3$
Transport	3.56745	—	—
P_1	3.56745	3.56733	6.0160
$P_{1/3}$	3.55436	3.55449	0.12301
Diffusion	3.45833	3.45826	1.4125
SP_2	4.49107	4.49137	3.1799
Improved SP_2	3.56745	3.56705	0.60744
SP_3 w/init. smoothing	4.49107	4.49112	1.7987
SP_3	4.49107	4.49138	2.6168
SSP_3 w/init. smoothing	3.45833	3.45757	5.7591
SSP_3	3.45833	3.45824	4.2273

approximation and the P_1 discretization have the highest error at this time, even though the flux-weighted average of $(x - x_a)^2$ for these methods is fairly accurate. Then at $t = 15$, Figure 7 and Table 6 show that once more the SP_2 approximation, both versions of the SP_3 approximation, the improved SP_2 approximation, and the P_1 discretization are the most accurate methods with respect to the scalar flux and the flux-weighted average of $(x - x_a)^2$, while the relative error in the $P_{1/3}$ approximation has increased substantially from $t = 5$.

TABLE 6 Theoretical and Numerical Values of $\langle (x - x_a)^2 \rangle_\phi$ and Error In the Scalar Flux for the Second Problem at $t = 15$.

Method	Theoretical $\langle (x - x_a)^2 \rangle_\phi$	Numerical $\langle (x - x_a)^2 \rangle_\phi$	$\|\|\phi_{\text{trans}} - \phi\|\|_2 \times 10^4$
Transport	13.050	—	—
P_1	13.050	13.050	0.35646
$P_{1/3}$	10.962	10.961	0.49504
Diffusion	10.125	10.125	0.82434
SP_2	14.003	14.003	0.26242
Improved SP_2	13.050	13.050	0.092725
SP_3 w/init. smoothing	14.003	14.003	0.16636
SP_3	14.003	14.003	0.19837
SSP_3 w/init. smoothing	10.125	10.124	1.3689
SSP_3	10.125	10.124	1.2734

We can make several general observations regarding the numerical results presented in this section. First, the predicted values for the flux-weighted average of $(x - x_a)^2$ agreed well with the observed numerical values for this quantity. However, an accurate flux-weighted average of $(x - x_a)^2$ did not always correspond to an accurate solution. It appears that requiring this flux-weighted average to be accurate is a necessary rather than sufficient condition for determining if a particular angular approximation method will produce accurate solutions. Nevertheless, the improved SP_2 approximation, which does preserve the correct flux-weighted average of $(x - x_a)^2$, was consistently one of the most accurate angular approximations for the problems we examined.

Before concluding this section, we feel that some further discussion concerning the behavior of the P_1 discretization is in order. Although this method also preserves the correct flux-weighted average of $(x - x_a)^2$, it was not particularly accurate for the two problems we considered. Indeed, it was the shortcomings of the P_1 discretization that motivated the development of alternate techniques such as the angular approximation methods we examined in this paper. The P_1 equations are the lowest order system that has the same flux-weighted averages of x and $(x - x_a)^2$ as the analytic transport equation. Unfortunately, capturing these quantities exactly with such a simplified system of equations leads to several idiosyncrasies, such as solutions that propagate at an incorrect speed. In the previous numerical results, this incorrect speed caused the odd behavior of the P_1 discretization.

7. Conclusions

We have extended moment analysis, a technique developed for investigating the accuracy of discrete-ordinates spatial discretization schemes, to time-dependent radiation transport and applied it to several angular approximation methods. Although restricted to infinite, homogeneous media, moment analysis is especially appropriate for examining the accuracy of these methods as they do not correspond to a sequence of increasingly accurate angular discretizations and therefore are not amenable to standard truncation analysis. We have shown that all of the methods preserve the correct flux-weighted average of x but not the correct flux-weighted average of $(x - x_a)^2$. In addition, we have demonstrated

that, for general cross sections and large elapsed time, the error in this latter quantity is smallest in magnitude for the SP_2 and SP_3 approximations. We have also presented a simple improvement to the SP_2 approximation that allows this method to produce the correct flux-weighted average of $(x - x_a)^2$.

With a set of numerical examples we have tested the results of our analysis. We found that, for each angular approximation method, the predicted value for the flux-weighted average of $(x - x_a)^2$ agreed well with the numerical value for this quantity. We further observed that an accurate flux-weighted average of $(x - x_a)^2$ was not always accompanied by an accurate solution. However, the angular approximation methods that produced the most accurate solutions also had the most accurate values for this flux-weighted average. In particular, the SP_2 and SP_3 approximations were two of the most accurate methods at large elapsed times, while the improved SP_2 approximation was one of the most accurate methods at all times, for the the problems we examined. Thus, we conclude that an accurate flux-weighted average of $(x - x_a)^2$ is a necessary, but not sufficient, condition for an overall accurate angular approximation method.

Acknowledgments

The work of the first author (J.D.D.) was performed under U.S. government contract DE-AC52-06NA25396 for Los Alamos National Laboratory, which is operated by Los Alamos National Security, LLC, for the U.S. Department of Energy.

References

Bornemann, F., Laurie, D., Wagon, S., Waldvogel, J. (2004). *The SIAM 100-Digit Challenge*. Philadelphia: Society for Industrial and Applied Mathematics.

Brantley, P. S., Larsen, E. W. (2000). Spatial and angular moment analysis of continuous and discretized transport problems. *Nucl. Sci. Eng.* 135:199.

Frank, M., Klar, A., Larsen, E. W., Yasuda, S. (2007). Time-dependent simplified P_N approximation to the equations of radiative transfer. *J. Comp. Phys.* 226:2289.

Ganapol, B. D. (2008). *Analytical Benchmarks for Nuclear Engineering Applications*. Paris: Nuclear Energy Agency.

Lewis, E. E., Miller, Jr., W. F. (1993). *Computational Methods of Neutron Transport*. La Grange Park, Illinois: American Nuclear Society.

Lewis, H. W. (1950). Multiple scattering in an infinite medium. *Phys. Rev.* 78:526.
McClarren, R. G., Evans, T. M., Lowrie, R. B., Densmore, J. D. (2008). Semi-implicit time integration for P_N thermal radiative transfer. *J. Comp. Phys.* 227:7561.
Olson, G. L. (2009). Second-order time evolution of P_N equations for radiation transport. *J. Comp. Phys.* 228:3072.
Olson, G. L., Auer, L. H., Hall, M. L. (2000). Diffusion, P_1, and other approximate forms of radiation transport. *J. Quant. Spectrosc. Radiat. Transfer* 64:619.
Simmons, K. H., Mihalas, D. (2000). A linearized analysis of the modified P_1 equations. *J. Quant. Spectrosc. Radiat. Transfer* 66:263.